Critical properties of quantum three- and four-state Potts models with boundaries polarized along the transverse field

N. Chepiga[1*],

1 Kavli Institute of Nanoscience, Delft University of Technology, Lorentzweg 1, 2628 CJ Delft, the Netherlands

* n.chepiga@tudelft.nl

September 6, 2021

Abstract

By computing the low-lying energy excitation spectra with the density matrix renormalization group algorithm we confirm the boundary conformal field theory predictions for the three-state Potts minimal model in 1+1D with boundaries polarized in the direction of the transverse field. We further show that the transverse-polarized boundary conditions lead to scale-invariant conformal towers of states at the critical point of the quantum four-state Potts model - a special symmetric case of the Ashkin-Teller model. Finally, we phenomenologically establish the duality between fixed and free, and between transverse-polarized and three-state-mixed boundary conditions at the four-state Potts critical point.

1 Introduction

Over the past decades boundary critical phenomena attracted a lot of interest in the context of statistical physics [1–3] and impurity problem [4–6] in condensed matter and particle physics. The presence of the boundary affects measurable observables and change energy spectra making the problem highly non-trivial [7, 8]. Many exact results for the simplest critical models have been predicted by the boundary conformal field theory [1, 2, 7, 9, 10].

The attention to the boundary critical phenomena has been re-attracted recently by the progress in numerical techniques for quantum many-body systems. Over the years, density matrix renormalization group (DMRG) algorithm [11–14] has established itself as one of the most powerful and accurate numerical tool for low-dimensional systems. Although DMRG is suitable for systems with either open or periodic boundary conditions, the latter has significantly higher computational costs. Thus, numerical investigation of the nature of quantum phase transitions often requires a theoretical understanding of the boundary critical phenomena. Traditionally, the universality class of the transition is identified numerically by computing critical exponents and the central charge. Both can be extremely sensitive to finite-size effects and affected by logarithmic corrections or possible crossovers. Excitation spectra at the conformal critical point are known to form a special structure - conformal towers of states - and contain more information about the underlying critical theory. Therefore, the catalog of the conformal towers of states for different critical theories and under various boundary conditions is essential for numerical investigation of quantum phase transitions.

For the critical transverse-field Ising model the exact correspondence between primary fields and various combinations of free and fixed boundary conditions has been worked out analytically by Cardy [2] and further confirmed numerically [15–18]. For the tri-critical Ising model Affleck [10] predicted partially-polarized boundary conditions to be conformally invariant and different from the free and fully-polarized ones. This prediction has been recently confirmed numerically in 1+1D [19] and 2+0D [18].

The three- and four-state Potts models are generalization of the transverse-filed Ising model to a system with local Hilbert space $d = 3$ and 4 respectively and can be defined by the Hamiltonian [20]:

$$H_{\text{Potts}} = -J \sum_{i=1}^{N-1} \sum_{\mu=1}^{d} P_i^{\mu} P_{i+1}^{\mu} - h \sum_{i=1}^{N} P_i, \tag{1}$$

where $P_i^{\mu} = |\mu\rangle_{ii}\langle\mu| - 1/d$ tends to project the spin at site i along the μ direction while $P_i = |\eta_0\rangle_{ii}\langle\eta_0| - 1/d$ tends to align spins along the direction $|\eta_0\rangle_i = \sum_{\mu} |\mu\rangle\sqrt{d}$. The first term in the Hamiltonian plays the role of the ferromagnetic interaction, while the second one is a generalized transverse field. The model is critical for $h = J$. For convenience, we label single-particle states for $d = 3$ by A, B and C. The boundary-field correspondence for free, fully-polarized (A, B or C), and mixed [3] (AB, AC or BC) boundary conditions has been established in the original work by Cardy [2]. Later, Affleck, Oshikawa and Saleur [21] have found that the fully-polarized boundary conditions are dual to the free ones and predicted the "new" conformally-invariant boundary conditions dual to the mixed ones. This completes the set of the conformally-invariant boundary conditions for the three-state Potts critical point [22]. Conformal tower of states with the "new" boundary conditions has been recently detected numerically in 2+0D by allowing negative entries in the boundary Bolzmann weight matrix [18].

However, there is a simpler physical realization of the new boundary conditions in quantum 1D chains. Based on the duality argument the new boundary conditions are stabilized by reverting the sign of the transverse field at the edges [21]. Moreover, it turns out that the new critical point is stable with respect to the magnitude of the boundary transverse field. In other words, according to the boundary conformal field theory the new boundary conditions could be realized when the edges are polarized in the direction of the transverse field. In the present paper we will provide the numerical evidence confirming this field-theory prediction.

Furthermore, relying on extensive numerical simulations we will show that the duality remains valid in the four-state Potts model. Based on our numerical results we predict the duality between free and fixed boundary conditions. Moreover, we will empirically establish the duality between the boundaries polarized in the direction of the transverse field and three-state-mixed boundary conditions, i.e. those where only one out of four single-particle states is excluded at the edges. This generalizes previous predictions on the duality to the four-state Potts model and provides a phenomenological starting point for boundary conformal field theory for a generic Ashkin-Teller critical theory.

The rest of the paper is organized as follows. In Section 2 we briefly review the numerical method used in the paper. In Section 3 we present the excitation spectra of the critical three-state Potts model with transverse-polarized boundary conditions. Section 4 is dedicated to the boundary critical phenomena in the four-state Potts model. In Section 4.1 we present conformal towers of states of the four-state Potts model with free and fixed boundary conditions and establish the duality between them. In Section 4.2 we present numerically extracted conformal towers of states of the four-state Potts model with transverse-polarized boundary conditions and show their duality with respect to the three-state mixed boundary conditions. In Section 4.3 we briefly present our numerical

results for two-state-mixed boundary conditions. The results are summarized and put in perspective in Sec.5.

2 The method

Our numerical simulations have been performed with an extended version of the DMRG algorithm explained in details in Ref. [15]. In this section we briefly review the main features of the algorithm and provide model-specific technical details.

The DMRG [11] algorithm has been originally designed to search for the ground-state. It provides an efficient low-entanglement approximation of quantum many-body state. The accuracy of the wave-function is controlled by the dimension D of the tensors - the number of basis vectors in the density matrix with the largest Schmidt values. Calculation of the excitation spectra is usually more involved. If the wave-function obeys some symmetry, and if the excited state of interest is the lowest energy state of some symmetry sector, then the energy of this state can be computed by running the ground-state DMRG within the corresponding sector. This is a common practice to compute magnetic excitations in spin chains [11, 23–25]. If, however, excitations cannot be distinguished by any symmetry, as in the case of the three- and four-state Potts models, the algorithm has to be modified significantly. There are three well established strategies. *i)* The density matrix is constructed not only from basis vectors that appear in the Schmidt decomposition of the ground state but mixed with the basis vectors that appear in the Schmidt decomposition of low-lying excitations [26–30]. In this case the bond dimension and the complexity increase very fast with the number of excitations, thus typically one targets five or fewer excited states [12]. *ii)* After constructing the ground-state in the matrix product state (MPS) representation, one can search for an eigenstate that is orthogonal to the ground state and has the smallest energy [14, 30, 31]. Higher excitations can also be accessed by looking for an eigenstate orthogonal to all previously constructed eigenvectors. By contrast to the first approach, the bond dimension remains small, but the algorithm has to be re-run for each eigenstate. *iii)* The third approach relies on the phenomenological observation that for critical systems an approximate basis constructed for the ground state is also suitable to describe the low-lying excited states [15]. By contrast to the first approach this method remains variational with respect to the ground-state. Well converged excitations appear as a flat modes as a function of DMRG iterations. The method has been benchmarked on the critical Ising and three-state Potts models for which the conformal towers with up to 30 states have been computed [15].

We use infinite-size DMRG with the bond dimension $D = 30$ to produce a guess wave-function and increase the bond dimension up to $D = 67$ in the warm-up sweep. In the following six sweeps we increase the bond dimension linearly with each half-sweep up to its maximal value $D_{\max} = 250$. This way we can easily track the convergence with respect to both the number of sweeps and the bond dimension D. When convergence cannot be reached for the chosen $D_{\max}$, typically this only happens for large system size and higher excitation levels, we still can get correct estimate of the spectra by extrapolating the energies. In Fig.1 we present one of the trickiest case - the critical four-state Potts model with free boundary conditions and $N = 100$.

In Fig.1**a** we show raw DMRG data for the energy spectrum as a function of DMRG iterations. A periodic increase of the excitation energies occurs close to the chain boundary and is the result of the reduced Hilbert space by MPS construction. The first excited state is three-fold degenerate (yellow and red symbols are almost completely hidden under the purple ones) and starting from the fourth sweep has a well converged energy reflected in

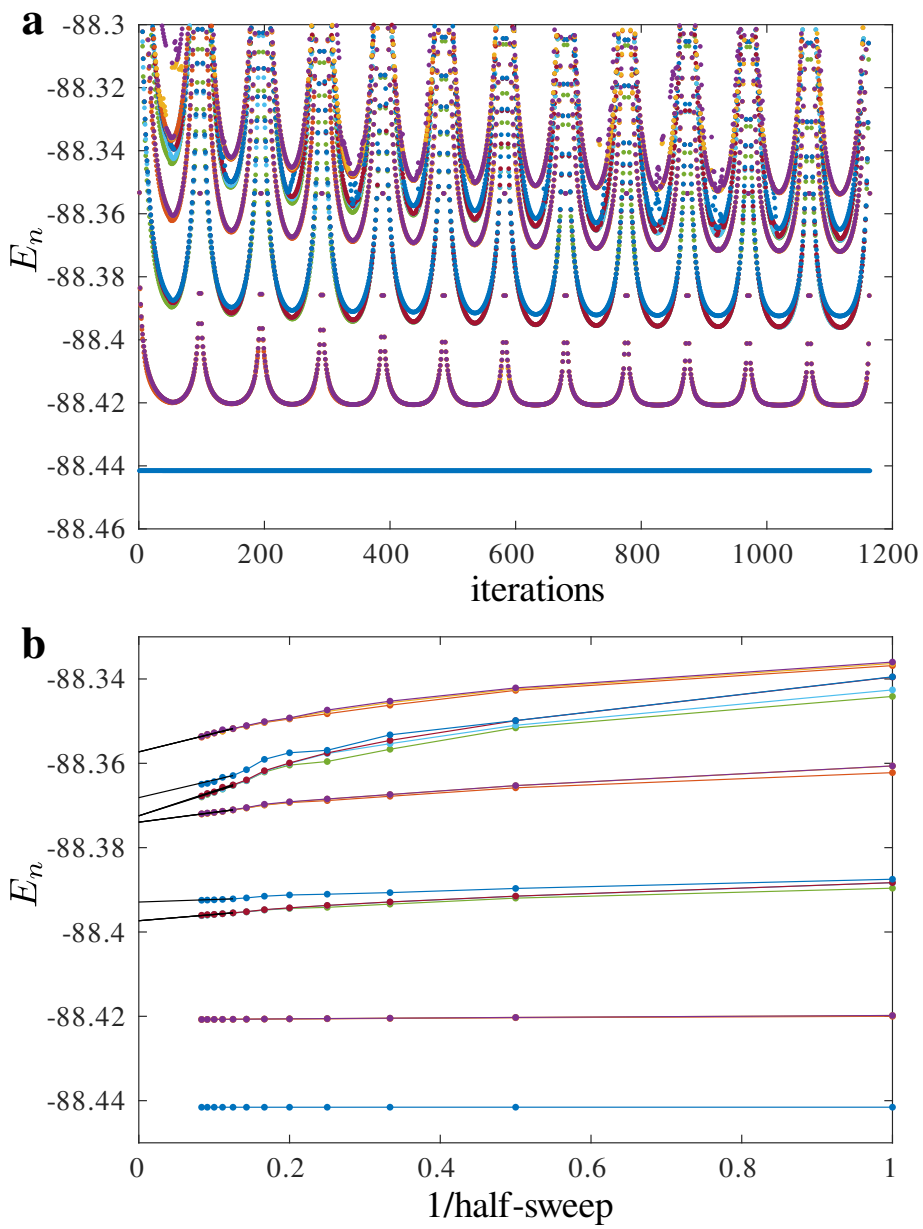

Figure 1: **a** Energy of the 19 low-energy states in the critical four-state Potts model with $N = 100$ sites as a function of iterations. The periodic increase of the energy occurs close to the chain boundary and is the result of the reduced Hilbert space by MPS construction. The flattening of the energies in the middle of the chain is an indicator of convergence. Non converged states are extrapolated towards infinite number of sweeps (equivalently infinite bond dimension) as shown in **b**. Note that many of the shown states are three-fold degenerate and some data points are completely hidden behind the others.

the flat intervals. The convergence of higher excitations is often slower. When convergence cannot be reached the results are obtained by extrapolating the value of the energy at the local minima towards infinite number of sweeps (or equivalently towards infinite bond dimension D). For extrapolation we use a linear fit of the last five points (black lines).

For the three-state Potts model we include only the converged results, without applying an extrapolation. For the four-state Potts model the extrapolation has been applied for higher energy levels for $N > 50$.

3 Transverse-polarized boundary conditions for three-state Potts critical point

Let us first focus on the three-state Potts model defined by the Hamiltonian 1 with $d = 3$. The critical point $h = J$ is described by the minimal model of conformal field theory with $(p, p') = (6, 5)$ and ten primary fields listed in A [32–34]. We realize fixed boundary condition A (B, or C) by applying a negative longitudinal field along the first (second, or third) component of the local Hilbert space, while positive longitudinal field along the same component allows to exclude this state and thus lead to a mixed boundary conditions BC (AC, AB). In order to realize the "new" boundary conditions predicted by Affleck at al. [21] we polarize the edges along the direction of the transverse field by setting up the field $h_1 = h_N = -10$ while keeping the transverse field in the bulk critical $h_i = J = 1$ for $2 \leq i \leq N-1$. Below we remind the list of the partition functions involving the new boundary conditions [21]:

$$Z_{\text{new,A}} = Z_{\text{new,B}} = Z_{\text{new,C}} = \chi_{2,2} + \chi_{3,2} \tag{2}$$

$$Z_{\text{new,AB}} = Z_{\text{new,BC}} = Z_{\text{new,AC}} = \chi_{1,2} + \chi_{4,2} + \chi_{2,2} + \chi_{3,2} \tag{3}$$

$$Z_{\text{new,free}} = \chi_{\epsilon} + \chi_{\sigma} + \chi_{\sigma}^{\dagger} \tag{4}$$

$$Z_{\text{new,new}} = \chi_{I} + \chi_{\epsilon} + \chi_{\sigma} + \chi_{\sigma}^{\dagger} + \chi_{\psi} + \chi_{\psi}^{\dagger}. \tag{5}$$

The structure of the conformal tower of states are given by the small-q expansion of the corresponding characters listed is the A. The final expression for each set of boundary conditions are provided below:

$$Z_{\text{new,A}} = q^{-1/30+1/40}\left(1 + q^{0.5} + q + q^{1.5} + 2q^2 + 2q^{2.5} + 3q^3 + 3q^{3.5} + 4q^4 + 5q^{4.5} + ...\right) \tag{6}$$

$$Z_{\text{new,AB}} = q^{-1/30+1/40}\left(1 + q^{0.1} + q^{0.5} + q + q^{1.1} + q^{1.5} + q^{1.6} + 2q^2 + q^{2.1} + 2q^{2.5} + q^{2.6} + 3q^3 + 2q^{3.1} + 3q^{3.5} + 2q^{3.6} + ...\right) \tag{7}$$

$$Z_{\text{new,free}} = q^{-1/30+1/15}\left(2 + q^{\frac{1}{3}} + 2q + 2q^{1\frac{1}{3}} + 4q^2 + 2q^{2\frac{1}{3}} + 6q^3 + 4q^{3\frac{1}{3}} + ...\right) \tag{8}$$

$$Z_{\text{new,new}} = q^{-1/30}\left(1 + 2q^{\frac{1}{15}} + q^{\frac{2}{5}} + 2q^{\frac{2}{3}} + 2q^{1\frac{1}{15}} + 2q^{1\frac{2}{5}} + 2q^{1\frac{2}{3}} + q^2 + 4q^{2\frac{1}{15}} + 2q^{2\frac{2}{5}} + 4q^{2\frac{2}{3}} + ...\right) \tag{9}$$

Let us briefly remind how conformal towers can be read-out form the small-q expansion. For example, let us consider the expansion for $Z_{\text{new,free}}$ given by Eq.8. There is a pre-factor that is the same for all towers and defined by the central charge c of the critical theory as $q^{-c/24}$. For the three-state Potts model $c = 4/5$ that results in $q^{-1/30}$. The second pre-factor is the smallest scaling dimension of the primary fields entering the tower. For $Z_{\text{new,free}}$ it is equal to $1/15$ - the dimension of the primary field σ. Since both, σ and $\sigma^{\dagger}$ enter the tower, the multiplicity of the corresponding levels are doubled, in particular, the

ground-state is two-fold degenerate which is reflected in the first term in the brackets. All other terms in the expansion are given in the form mq^n, where m reflects the multiplicity of the energy level n.

In order to extract conformal towers numerically, we compute low-lying energy spectra with up to 21 energy levels. According to the conformal field theory, energy gap scales as $E_n - E_0 = \pi v n/N$, where N is the system size and v is a non-universal sound velocity. For the three-state Potts model defined by the Hamiltonian 1 the value of the velocity has been computed numerically $v \approx 0.857$ [15] and will be used throughout this section. Our numerical results for the four conformal towers involving transverse-polarized boundary conditions are presented in Fig.2. Given that there are no fitting parameters the agreement between the theory (colored lines) and the numerical data (blue symbols) is extremely good. One can notice that some conformal towers ($\chi_{2,2}$, $\chi_{3,2}$, σ, ϵ) are affected by finite-size effects stronger than the other (I, ψ, $\chi_{1,2}$, $\chi_{4,2}$). This effect has been observed before for fixed, free and mixed boundary conditions [15].

To summarize this section, conformal towers of states predicted by Affleck at al. [21] for the new boundary conditions appear in a quantum 1D version of the critical three-state Potts model with boundaries polarized in the direction of the transverse field. This provides a more physical and intuitive realization of the new boundary conditions in quantum chains than in the classical 2D model that requires negative entries in the boundary Bolzmann weight matrix.

4 Boundary critical phenomena in four-state Potts model

Boundary phenomena at the four-state Potts critical point are far less understood. The four-state Potts model defined by the Hamiltonian 1 is a straightforward generalization of the three-state Potts model to four-dimensional local Hilbert space. On the other hand, the four-state Potts critical point is a special symmetric point of a generic Ashkin-Teller critical theory [35]. An effective quantum Ashkin-Teller model can be defined by the following microscopic Hamiltonian:

$$H_{\text{Ashkin-Teller}} = -J \sum_{i=1}^{N-1} \left[\frac{1+\lambda}{2} \sum_{\mu=1}^{d} P_i^{\mu} P_{i+1}^{\mu} - \frac{1-\lambda}{2} (P_i^1 P_{i+1}^4 + P_i^2 P_{i+1}^3 + \text{h.c.}) \right] - h \sum_{i=1}^{N} P_i(\lambda), \quad (10)$$

where λ is the Ashkin-Teller parameter and

$$P_i(\lambda) = \frac{1}{4} \begin{pmatrix} 0 & 1 & 1 & \lambda \\ 1 & 0 & \lambda & 1 \\ 1 & \lambda & 0 & 1 \\ \lambda & 1 & 1 & 0 \end{pmatrix}.$$

The model coincide with the four-state Potts model given by Eq.1 for $\lambda = 1$. For $\lambda = 0$ the model is a quantum version pf the four-state clock model and corresponds to two decoupled Ising chains. Along the $J = h$ line the model is described by the Ashkin-Teller critical theory with central charge $c = 1$ and critical exponents varying continuously with λ. The operator content and partition functions on a torus have been analyzed by Yang [36]. Boundary critical phenomena for the special case of $\lambda = 0$ have been studied recently in

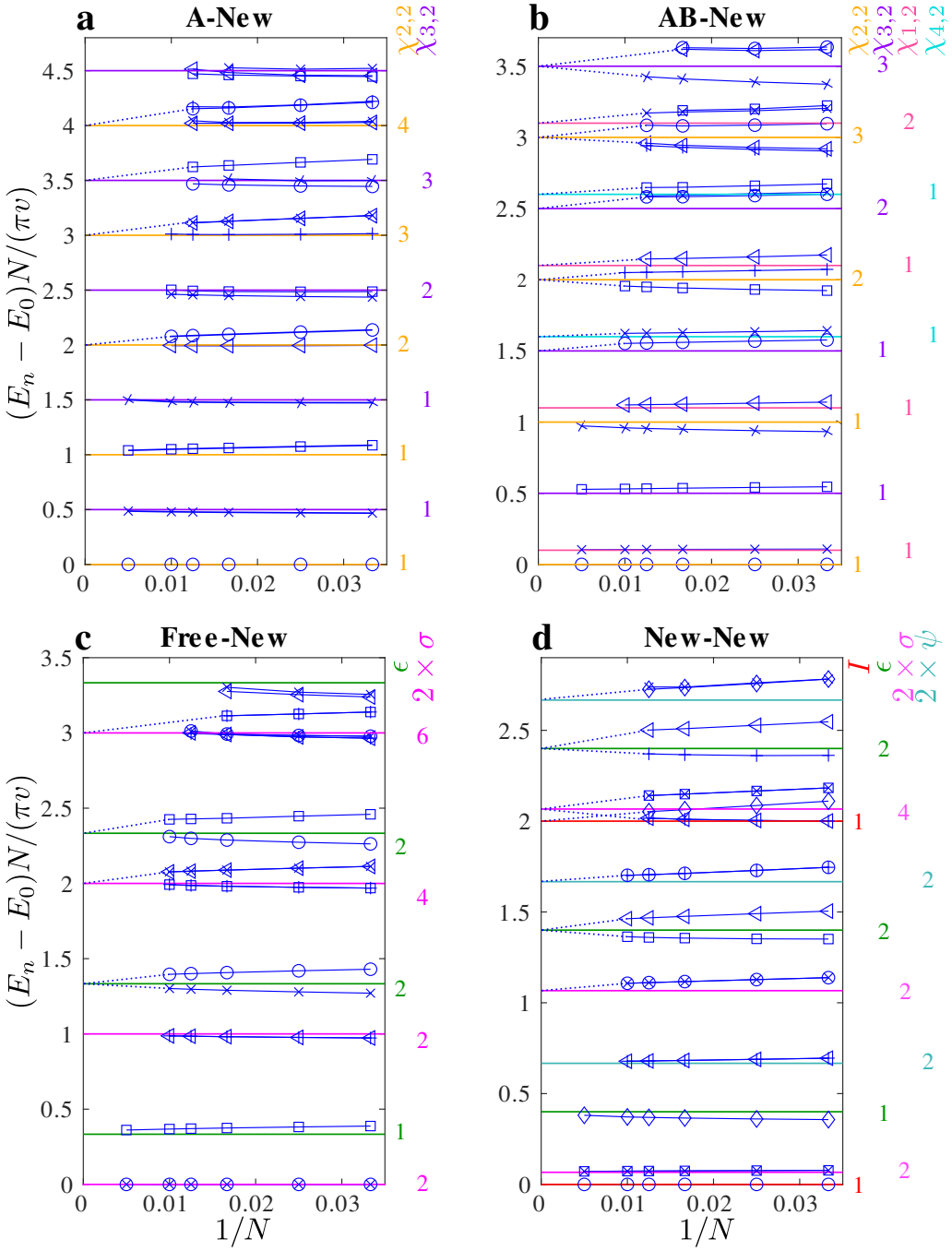

Figure 2: Conformal towers of states of the critical three-state Potts model with one edge polarized along the transverse field direction (following Ref. [21] we use the notation 'new') and the second edge is (a) fixed to one of the three single-particle states; (b) mixed between the two single-particle states; (c) free; (d) also polarized along the transverse field. The velocity is fixed to the value $v \approx 0.857$ reported in Ref. [15]. Blue symbols correspond to our DMRG data (different symbols are chosen to clarify multiplicities), lines of different colors correspond to different primary fields in the tower and listed on the right. The numbers under each character show the expected multiplicities of the levels and always match our numerical data. Blue dotted lines are guide to the eyes indicating where the energy levels are expected to end in the thermodynamic limit and for infinite DMRG bond dimension D.

the context of a defect line in two-dimensional Ising model [37]. The conformal tower of states as a function of $\lambda \in [0, 1]$ for fixed and symmetric boundary conditions A-A has been reported recently in Ref. [38].

There are two challenges associated with numerical investigation of the conformal towers of the Ashkin-Teller model. First, by contrast to the Ising and 3-state Potts minimal models, there are logarithmic corrections present in the Ashkin-Teller critical theory which might significantly affect numerical results. Second, there is an infinite number of primary fields in the generic Ashkin-Teller model. The goal of this section is to identify which of the primaries appear at the four-state Potts point for a set of common boundary conditions.

4.1 Free and fixed boundary conditions in the four-state Potts model

Following the notations of the previous section we label single-particle states for $d = 4$ by A, B, C and D. We start our investigation with the the simplest case - fixed and symmetric boundary conditions A-A (obviously, due to symmetry in the model the results for B-B, C-C, and D-D boundary conditions will be the same). By analogy with the Ising and the three-state Potts models, we expect the low-energy spectra to be described by an identity conformal tower. Although from Eq.30 for the three-state Potts model we know that more than one character might enter the identity tower (and that is indeed what we observe numerically for $d = 4$). In any case, the smallest dimension of the primaries is expected to be $x = 0$. The Virasoro character of this primary field is given by:

$$\chi_0 = (1-q)\left[q^{-1/24}\left(1+q+2q^2+3q^3+5q^4+7q^5+11q^6+...\right)\right] \\ = q^{-1/24}(1+q^2+q^3+2q^4+2q^5+4q^6+...), \quad (11)$$

where the term in the square brackets is a small-q expansion of the Dedekind function. The resulting expansion has the structure distinct for 0-dimensional characters of the minimal models: the first order term in q is absent. There is a non-universal parameter in the critical theory - the sound velocity v. We extract the velocity from the lowest energy gap in a chain with A-A boundary condition and get the value $v = \Delta EN/(2\pi) \approx 0.785$. We will use this value through the rest of this section.

In Fig.3**a** we present our numerical data for the conformal towers of states obtained with A-A boundary conditions. At the integer levels we recover the structure and multiplicities of χ_0 given by Eq.11. In addition, above $n = 3$ we detect the presence of another, double-degenerate primary with the scaling dimension $x \approx 3.5$. In order to identify the scaling dimension numerically we extrapolate the lowest level of the tower to the thermodynamic limit (dotted red line) and estimate the error-bar as a difference between the extrapolated value and the last available data point (here $N = 100$). The resulting estimate for the scaling dimension is $x \approx 3.52 \pm 0.03$. Moreover, we empirically extract the structure of the tower and get:

$$\chi_{x\approx 3.5} = q^{-1/24+3.5}(1+q+2q^2+...), \quad (12)$$

This structure agrees with the character of the Virasoro algebra for $x \neq k^2/4$ ($k \in \mathbb{Z}$) [36]. To summarize, the partition function of an open chain with fixed symmetric boundary conditions A-A is given by:

$$Z_{A-A} = \chi_0 + 2 \times \chi_{3.5} + ..., \quad (13)$$

where three dots indicate that additional entries of primary fields with scaling dimension $x > 6$ cannot be excluded by our numerical analysis.

So far we assumed the lowest scaling dimension of the tower to be zero. Let us now provide numerical argument supporting this hypothesis. According to conformal field theory the ground-state energy E_0 of a chain with open boundary conditions are expected to scale with the system size N as:

$$E_0 = \varepsilon_0 N + \varepsilon_1 + \left(-\frac{1}{24} + x\right)\frac{\pi v}{N}, \tag{14}$$

where ε_0 and ε_1 are non-universal constants. By fixing the sound velocity to the value $v \approx 0.785$, we fit our numerical data as shown in Fig.3**c**. The numerically extracted value of the scaling dimension $x < 5\times10^{-3}$ is in excellent agreement with our expectation $x = 0$.

Now, let us consider a non-symmetric combination of the fixed boundary conditions A-B (equivalent to A-C, B-C, etc. - six combinations in total). We start by fitting the scaling of the ground-state energy in the form of Eq.14. The results of the fit is presented in Fig.3**d**. By fixing the value of the velocity to $v \approx 0.785$, we extract the scaling dimension of the primary field to be $x \approx 0.822$. This points towards possible candidate of the primary field with $x = 5/6 \approx 0.833$. This implies that the scaling dimension $x \neq k^2/4$ ($k \in \mathbb{Z}$) and, according to Yang [36], the character with $x \approx 0.822$ is given by $q^{-1/24+x}(1 + q + 2q^2 + 3q^3 + 5q^4 + 7q^5 + ...)$. In Fig.3**b** we present our numerical results for the confromal tower of states with A-B boundary conditions. Energy levels up to $n = 2$ are in excellent agreement with the CFT predictions, especially given that there is no adjustment parameter: the only non-universal value is the sound velocity that we fix at $v \approx 0.785$ extracted from the A-A tower. However, the multiplicities of the states ending at the levels above $n = 2$ do not match the expansion. There are two possible explanations. On the one hand, some states might be affected by log-corrections stronger than others. In this case, one can imagine that intermediate levels of the tower detected at $n \approx 2.7, 3.7, 4.7$ will eventually end up at $n = 3, 4, 5$ respectively. This will restore the correct multiplicity for the higher levels, in particular $3q^3$ and $5q^4$. On the other hand, the finite-size extrapolation of the lowest intermediate level (dotted line) suggests that the energy level is at $n \approx 2.68 \pm 0.03$. If there is an additional primary field entering the tower and responsible for these intermediate state, its dimension would be $x \approx 2.68 + 0.822 \approx 3.50$ - the same as the dimension of the primary entering the A-A tower. Moreover, the multiplicities of the available three levels identified in A-A towers and summarized in Eq.12 match the multiplicities observed in the A-B tower. Therefore, our prediction for the A-B tower is the following:

$$Z_{A-B} = \chi_{5/6} + \chi_{3.5} + ..., \tag{15}$$

with

$$\chi_{5/6} = q^{-1/24+5/6}(1 + q + 2q^2 + 2q^3 + 4q^4 + ...) \tag{16}$$

Let us now study the conformal tower of a chain with free boundary conditions at both ends. By analogy with the Ising and the three-state Potts models we expect the duality between fixed and free boundary condition. From a dual point of view [21] the partition functions at low energies satisfy:

$$Z_{Free-Free} = Z_{A-A} + Z_{A-B} + Z_{A-C} + Z_{A-D}. \tag{17}$$

Since $Z_{A-B} = Z_{A-C} = Z_{A-D}$, and using Eqs.13 and 15 we end up with the following prediction:

$$Z_{Free-Free} = \chi_0 + 3 \times \chi_{5/6} + 5 \times \chi_{3.5} + ... \tag{18}$$

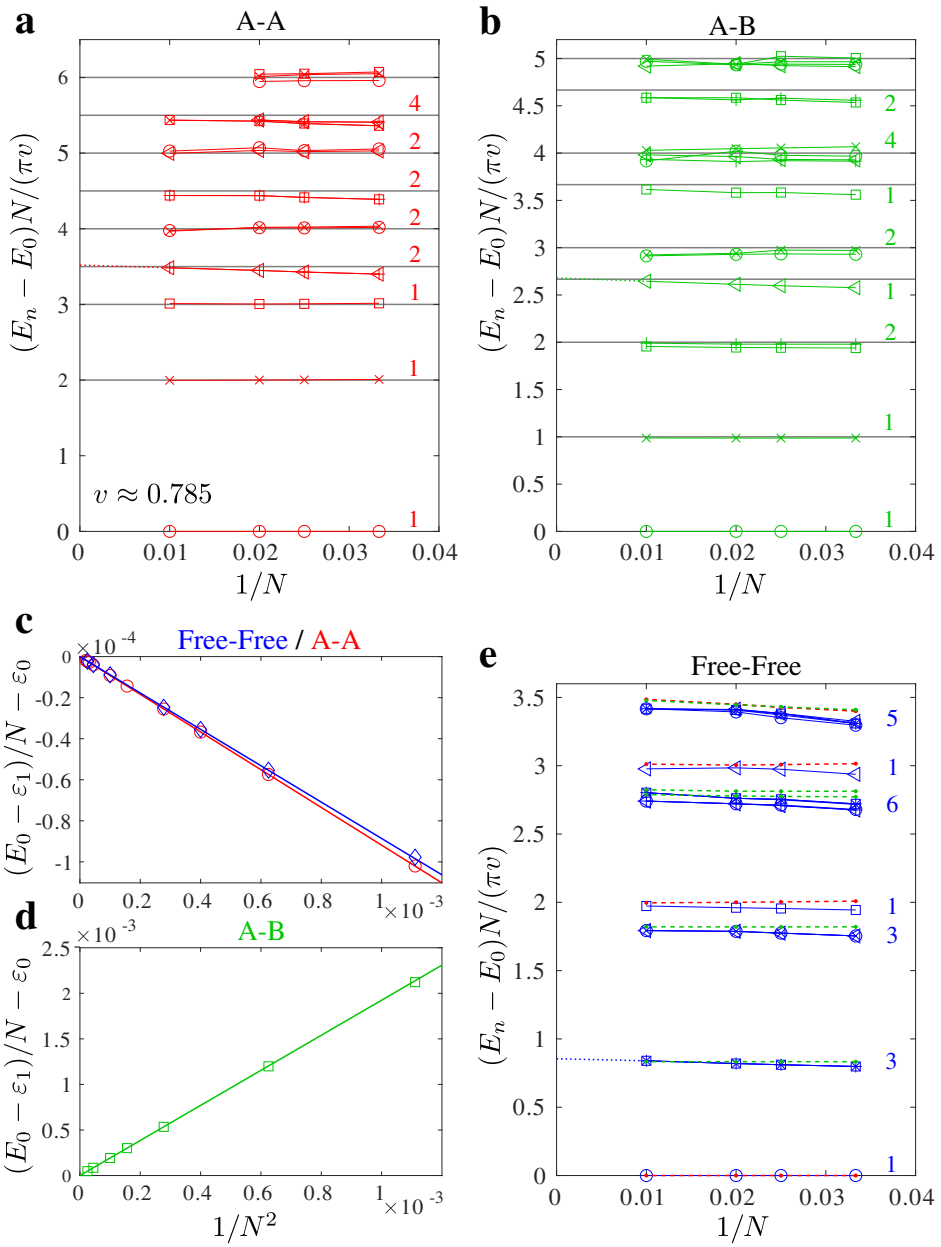

Figure 3: Conformal towers of states of the four-state Potts model with **a** fixed symmetric and **b** antisymmetric and **e** free boundary conditions. Symbols are DMRG data point extracted from the low-lying energy excitation spectra with velocity $v \approx 0.785$ computed from the lowest energy gap in **a**. Gray lines are the expected levels of conformal towers (see main text). In **e** the results from **a** (dashed red) and **b** (dashed green) are shown as a reference, the latter is shifted by $x = 5/6$. The dotted blue line is a finite-size extrapolation, the obtained value $n \approx 0.855$ is in good agreement with $x = 5/6$. The numbers on the right side of the towers indicate the multiplicity of each energy level. **c-d** Finite-size scaling of the universal part of the ground-state energy fitted with Eq.14. Solid lines are the results of the fit. **c** For fixed A-A and free boundary conditions the extracted scaling dimension agrees within 5×10^{-3} with the expected value $x = 0$. **d** For the fixed A-B boundary conditions the scaling dimension extracted numerically $x \approx 0.822$ is in good agreement with $x = 5/6$.

The small-q expansion then takes the form:

$$Z_{Free-Free} = q^{-1/24}\left(1 + 3q^{\frac{5}{6}} + 3q^{1\frac{5}{6}} + q^2 + 6q^{2\frac{5}{6}} + q^3 + 5q^{3.5} + 6q^{3\frac{5}{6}} + 2q^4 + 5q^{4.5} + ...\right) \quad (19)$$

This prediction is in excellent agreement with our numerical data presented in Fig.3**e**. From finite-size scaling of the ground-state energy presented in Fig.3**c** we get the smallest scaling dimension to be $x < 5 \times 10^{-3}$ which is in good agreement with the expected value $x = 0$. There are three cross checks available at this stage. First, on top of the Free-Free conformal tower in Fig.3**e** we plot our raw DMRG results for A-A (dashed red lines) and for A-B (dashed green lines) towers, shifting the latter by 5/6. The excellent agreement between these results confirms the duality. Second, by extrapolating the first excited state of the Free-Free tower we get $n \approx 0.855$ which is in a good agreement with the scaling dimension 5/6 obtained for the A-B tower. Finally, the almost perfect collapse of the five-fold degenerate state at $n \approx 3.5$ in the Free-Free tower strongly supports the presence of $x = 3.5$ primary field in both, A-A and A-B, towers.

4.2 Transverse-polarized and three-state-mixed boundary conditions

Let us now consider the boundary conditions where one state, say D, is suppressed at the edge, which leads to the three-state-mixed boundary condition ABC. If the same local single-particle state is suppressed at both edges, we end up with symmetric boundary conditions ABC-ABC (equivalently ABD-ABD, etc). If the suppressed states are different then boundary conditions would be ABC-ABD (equivalent to ABC-ACD, etc). Our numerical results for conformal towers for these boundary conditions are presented in Fig.4**a-b**. We expect an identity tower given by Eq.11 to appear for all symmetric boundary conditions, including ABC-ABC. This agrees with the absence of the $n = 1$ level in Fig.4**a**. The presence of the identity tower is further confirmed by the finite-size scaling of the ground-state energy presented in Fig.4**c** where the numerically extracted scaling dimension agrees within 2×10^{-3} with $x = 0$. On top of the identity tower we see the presence of a double degenerate primary with dimension $x \approx 0.64 \pm 0.03$ extracted from the lowest level of the tower (dotted line). In addition, there is a primary with scaling dimension $x \approx 1.33 \pm 0.03$(dash-dotted line). Numerical results might look a bit messy around $n \approx 2.5$ because of the level crossing of a non-degenerate energy level going down towards $n \approx 2.33$ and four-fold degenerate states going up towards $n \approx 2.64$.

The partition function is then given by:

$$Z_{ABC-ABC} = \chi_0 + 2 \times \chi_{x\approx 0.64} + \chi_{x\approx 1.33} + ... \quad (20)$$

Numerical results for the tower with non-symmetric three-state-mixed boundary conditions ABC-ABD is shown in Fig.4**b**. We do not expect the identity primary field to enter this tower, therefore we naturally expect to observe an energy level at $n = 1$. Most likely this is the state shown with green crosses and shifted above $n = 1$ by some finite-size effects. In other words, the effective velocity of this tower and for accessible system sizes is $v \approx 0.85$ which is about 8% higher than the estimate we got from the A-A tower. This is not very uncommon and large deviation in the velocity has been reported for AB-AC boundary conditions in the three-state Potts model [39]. We normally extract the scaling dimension of the lowest state of the tower by analyzing the universal term of the ground-state energy. However, as shown in Fig.4**d** the data points are of the order 10^{-7} and are non-monotonous. This suggests that $(-1/24 + x)$ is extremely small (below 10^{-3}). We then may assume that the scaling dimension of the lowest primary is $x = 1/24$ or very

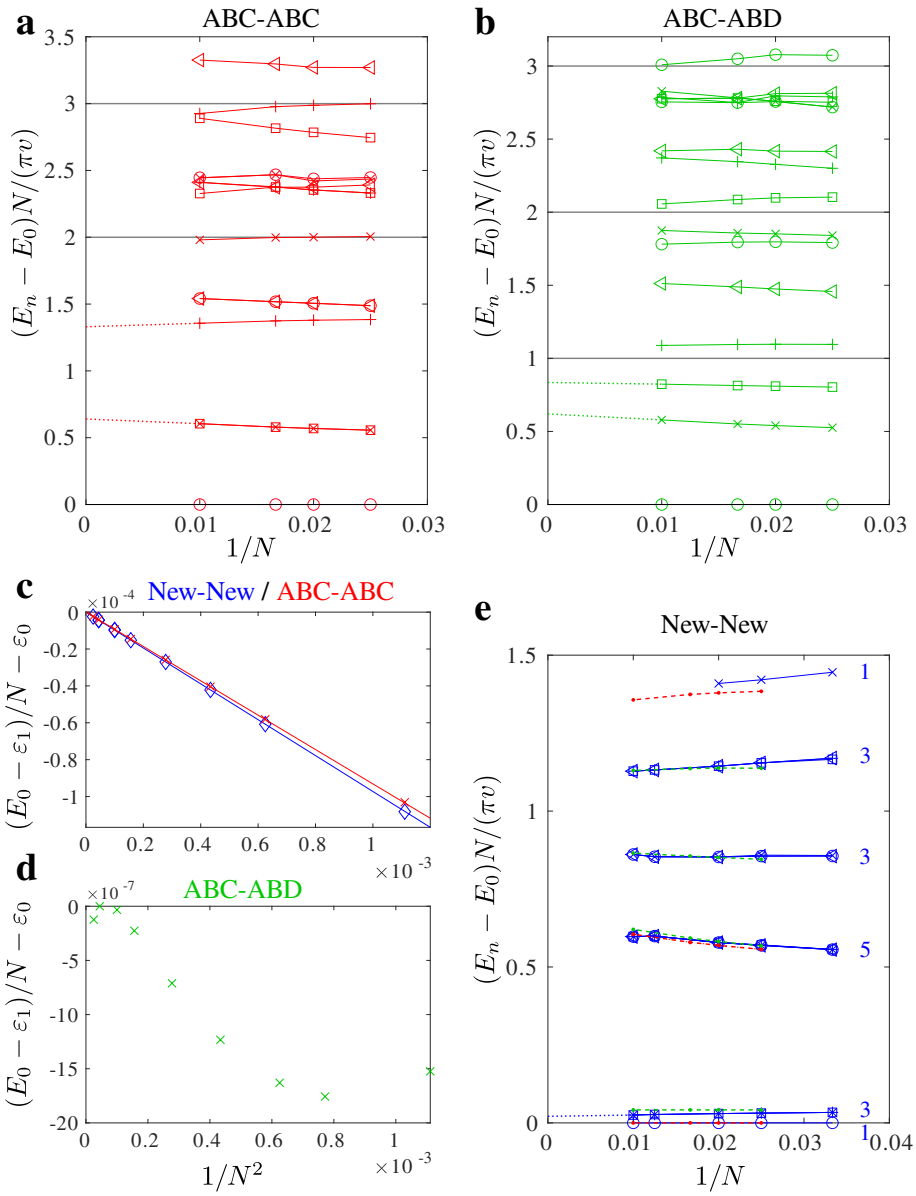

Figure 4: Conformal towers of states of the four-state Potts model with **a** three-state-mixed symmetric and **b** three-state-mixed non-symmetric boundary conditions, and **e** with boundaries polarized in the direction of the transverse field (following Ref. [21] we use the term "new" boundary conditions). Symbols are DMRG data points extracted from the low-lying energy excitation spectra with velocity $v \approx 0.785$. Gray lines are expected levels of conformal towers with the smallest scaling dimension. In **e** the results from **a** (dashed red) and **b** (dashed green) are shown as a reference, the latter is shifted by $x = 1/24$. Dotted lines are finite-size extrapolation with quadratic polynomial in $1/N$. **e** The numbers on the right side of the towers indicate the multiplicity of each energy level. **c-d** Finite-size scaling of the universal part of the ground-state energy fitted with Eq.14. **c** For ABC-ABC and New-New boundary conditions the extracted scaling dimension agrees within 4×10^{-3} with an expected value $x = 0$. **d** For the fixed ABC-ABD boundary conditions the scaling dimension of the primary field is close to $x = 1/24$ resulting in the data points of the order of 10^{-7}.

close to this value. Below $n = 1$ we observe two more levels of the towers, which means that the partition function has at least three primaries. The numerically estimated scaling dimension is $x \approx 1/24 + 0.64 \pm 0.04 \approx 0.68 \pm 0.04$ and $x \approx 1/24 + 0.835 \pm 0.01 \approx 0.88 \pm 0.01$. Note that the error bar mentioned here does not include the possible 8% error in the sound velocity. The partition function takes the following form:

$$Z_{ABC-ABD} = \chi_{x\approx 1/24} + \chi_{x\approx 0.68} + \chi_{x\approx 0.88} + ... \tag{21}$$

In the three-state Potts model mixed boundary conditions AB, AC and BC are dual to the new boundary conditions realized, as we have shown in the previous section, by polarizing edges along the transverse field. Assuming that this duality holds for the four-state Potts model, we expect

$$Z_{new-new} = Z_{ABC-ABC} + Z_{ABC-ABD} + Z_{ABC-ACD} + Z_{ABC-BCD}, \tag{22}$$

where due to symmetry the last three terms have the same conformal towers. The resulting partition function is given by:

$$Z_{new-new} = \chi_0 + [2 \times \chi_{x\approx 0.64} + 3 \times \chi_{x\approx 0.68}] + 3 \times \chi_{x\approx 1/24} + 3 \times \chi_{x\approx 0.88} + \chi_{x\approx 1.33} + ... \tag{23}$$

Numerical results for the conformal tower of states with both edges polarized in the direction of the transverse field is presented in Fig.4**e**. The raw DMRG data for ABC-ABC (red dashed line) and ABC-ABD (green dashed line) are shown as a reference, the latter is shifted by 1/24. Excellent agreement between the towers strongly supports the duality between the transverse-polarized (new) boundary conditions and the three-state mixed ones. There are two observations that can be made here. First, the lowest excitation energy in the New-New tower extrapolates to $n \approx 0.021 \pm 0.06$ which is two times smaller than $x = 1/24$ obtained from the ground-state energy scaling. Thus more accurate, perhaps analytical, methods are necessary to make a reliable prediction for the scaling dimension in this case. Second, the almost perfect five-fold degeneracy observed for $n \approx 0.64$ suggests that the two characters detected in ABC-ABC tower with $x \approx 0.64$ and in ABC-ABD tower with $x \approx 0.68$ refer to the same primary field present in all three towers shown in Fig.4. This points towards $x = 2/3$ as a possible candidate, while $x \approx 1.33$ is consistent with 4/3. Then our prediction for the new-new conformal tower is the following:

$$Z_{new-new} = \chi_0 + 3 \times \chi_{1/24} + 5 \times \chi_{2/3} + 3 \times \chi_{x\approx 0.88} + \chi_{4/3} + ... \tag{24}$$

For completeness, let us now consider the set of mixed boundary conditions, i.e. those, where left and right edges of the chain are described by different classes of boundary states. Based on the established duality between free and fixed and between three-state-mixed and transverse-polarized boundary conditions, we expect:

$$Z_{A-New} = Z_{Free-ABC} \tag{25}$$

and

$$Z_{Free-New} = Z_{A-ABC} + Z_{A-ABD} + Z_{A-ACD} + Z_{A-BCD}. \tag{26}$$

Eq.25 can be verified by a direct comparison of the two towers as presented in Fig.5. The scaling dimension extracted from the finite-size scaling of the universal term in the ground-state energy in Fig.5**a** for both towers is $x \approx 0.0204$ and points towards the primary field with $x = 1/48$. Direct comparison between the excitation spectra for A-New and ABC-Free boundary conditions presented in Fig.5**b** is spectacular given that there is no adjustment parameter between the towers. Likely, non-degenerate levels just below and

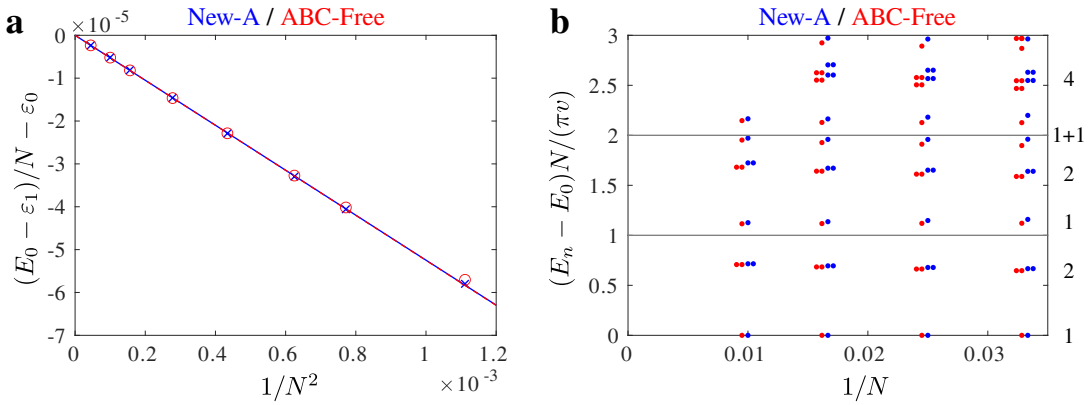

Figure 5: Direct comparison of the conformal tower of states with A-New (blue) and Free-ABC (red) boundary conditions. **a** Finite-size scaling of the universal part of the ground-state energy; the agreement is excellent and the numerically extracted value of the scaling dimension $x \approx 0.0204$ is in good agreement with $x = 1/48$. **b** Conformal towers of states extracted from the excitation spectra with A-New (blue) and Free-ABC (red) boundary conditions. For clarity some data points are shifted horizontally by up to 10^{-3}. The multiplicity of each level is marked with integer numbers on the right side of the panel.

just above $n = 2$ become degenerate in the thermodynamic limit, in agreement with the standard structure of the character of the Virasoro algebra for $x \neq k^2/4$ ($k \in \mathbb{Z}$) [36]: $\chi_{x=1/48} = q^{-1/24+1/48}(1 + q + 2q^2 + 3q^3...)$. On top of the $x = 1/48$ one can detect the presence of a double-degenerate primary with $x \approx 1/48 + 0.75 \pm 0.04 \approx 0.77 \pm 0.04$, so the partition functions contain:

$$Z_{A-New} = Z_{Free-ABC} = \chi_{x=1/48} + 2 \times \chi_{x\approx 0.77} + ... \tag{27}$$

In order to verify Eq.26, we compute the towers with Free-New, A-BCD and A-ABC boundary conditions. Due to symmetry the latter is equivalent to A-ACD and A-ABD. Our numerical results for this set of boundary conditions are summarized in Fig.6. From the finite-size scaling of the universal term in the ground-state energy (see Fig.6**c**) we obtain the scaling dimension to be $x \approx 0.124$ for A-ABC pointing towards the primary with $x = 1/8$. Scaling dimension obtained with A-BCD boundary condition in Fig.6**d** is $x \approx 0.43$. The structure of the excitation spectrum with A-ABC boundary conditions is presented in Fig.6**a**. The tower is significantly perturbed by finite-size and presumably by logarithmic corrections. If we assume, that the primary with $x = 1/8$ has the standard structure $\chi_{x=1/8} = q^{-1/24+1/8}(1 + q + 2q^2 + 3q^3...)$ then one can clearly distinguish the presence of another primary with the scaling dimension extracted from its lowest level (dotted red line) to be $x \approx 1/8 + 1.64 \pm 0.05 \approx 1.77 \pm 0.05$. For A-BCD on top of the $x \approx 0.43$ primary with $\chi_{x\approx 0.43} = q^{-1/24+0.43}(1 + q + q^2 + 2q^3...)$ we detect the two-fold degenerate primary with $x \approx 0.43 + 1.42 \pm 0.08 \approx 1.85 \pm 0.08$ (dotted green line). Among A-ABC and A-BCD towers, the ground-state scaling dimension is the smallest for A-ABC and equal to $x = 1/8$. We therefore expect the ground-state of the Free-New tower to have the same scaling dimension. The value $x \approx 0.125$ obtained numerically by fitting the ground-state energy (Fig.6**c**) is in excellent agreement with our expectation. Furthermore, because $Z_{A-ABC} = Z_{A-ABD} = Z_{A-ACD}$ the ground-state of the New-Free tower is expected to be three-fold degenerate. This is in excellent agreement with our numerical results presented in Fig.6**e**. On top of the New-Free tower we draw the raw DMRG data for A-ABC (red dashed lines) and A-BCD (green dashed lines), shifting the latter by $0.43 - 1/8 = 0.305$.

The agreement between them is perfect which once again confirms the prediction made in Eq.26 and the duality in general. Furthermore, by extrapolating the lowest excitation energy we obtain the value of the primary $x \approx 1/8 + 0.22 \pm 0.03 \approx 0.35 \pm 0.03$ significantly smaller than 0.43. This value also suggests that the primary with $x \approx 1.64 + 1/8 \approx 1.77$ in A-ABC tower and the primary with $x \approx 1.42 + 0.35 \approx 1.77$ in A-BCD tower corresponds to the same operator, which is further supported by the five-fold degeneracy detected around $n \approx 1.64$ in the New-Free tower in Fig.6**e**.

4.3 Two-state-mixed boundary conditions

For completeness let us also consider the two-state-mixed boundary conditions, i.e. those when only two single-particle states are allowed at the edges. Numerically we achieve this by applying equal longitudinal fields simultaneously along two directions at the edges. When the pair of components along which we apply the field is the same on both edges, we will call this boundary conditions AB-AB. When only one component coincides, we will refer to these boundary conditions as AB-AC. When the two pairs of components do not overlap we end up with the AB-CD boundary conditions.

Our numerical results for these boundary conditions are summarized in Fig.7. In the symmetric AB-AB case we clearly resolve the identity tower that according to our results for the A-A tower is composed of $\chi_0 + 2 \times \chi_{3.5}$ (see Eq.13). On top of the identity tower we detect the primary with $x \approx 0.21 \pm 0.01$ (dotted line) with an empirically extracted character expansion:

$$\chi_{x \approx 0.21} = q^{-1/24+0.21}(1 + 2q + 2q^2 + 4q^3 + ...). \tag{28}$$

There is yet another double-degenerate primary that appears around $n \approx 2.5$ and judging by higher levels it is severely affected by finite-size effects and/or log-corrections.

The lowest scaling dimension extracted from the ground-state scaling in the AB-AC tower is equal to $x \approx 0.0625$, which is in excellent agreement with the "stable" scaling dimension 1/16 that remains the same for a generic Ashkin-Teller critical theory even away from the four-state Potts point and corresponds to the magnetization (or spin) operator σ. The character of this operator obeys the standard form:

$$\chi_{x \approx 1/16} = q^{-1/24+1/16}(1 + q + 2q^2 + 3q^3 + ...). \tag{29}$$

On top of the $x = 1/16$ primary, we detect the presence of another primary with $x \approx 1/16 + 0.54 \pm 0.01 \approx 0.60$. This can point towards another magnetization operator with $x = 9/16$, however this hypothesis requires further analytical confirmation.

Finally, the lowest state in AB-CD tower is described by the primary with $x \approx 0.378$, which is sufficiently close to $x = 3/8$. On top of it, we detect the presence of the double-degenerate primary with $x \approx 0.378 + 0.67 \pm 0.1 \approx 1.04 \pm 0.01$. A possible candidate would be the primary with $x = 25/24$. Interestingly enough, slightly below the double degenerate level at $n \approx 1.67$, a non-generate state appears, indicating the presence of yet another primary with $x \approx 0.378 + 1.62 \pm 0.02 \approx 2.0 \pm 0.02$.

5 Discussion

In the first part of the paper we have provided numerical evidences that the "new" boundary conditions predicted with boundary conformal field theory by Affleck et al. [21] can be realized in the quantum version of the three-state Potts model by polarizing the edges in the direction of the transverse field. This complements previous DMRG results for

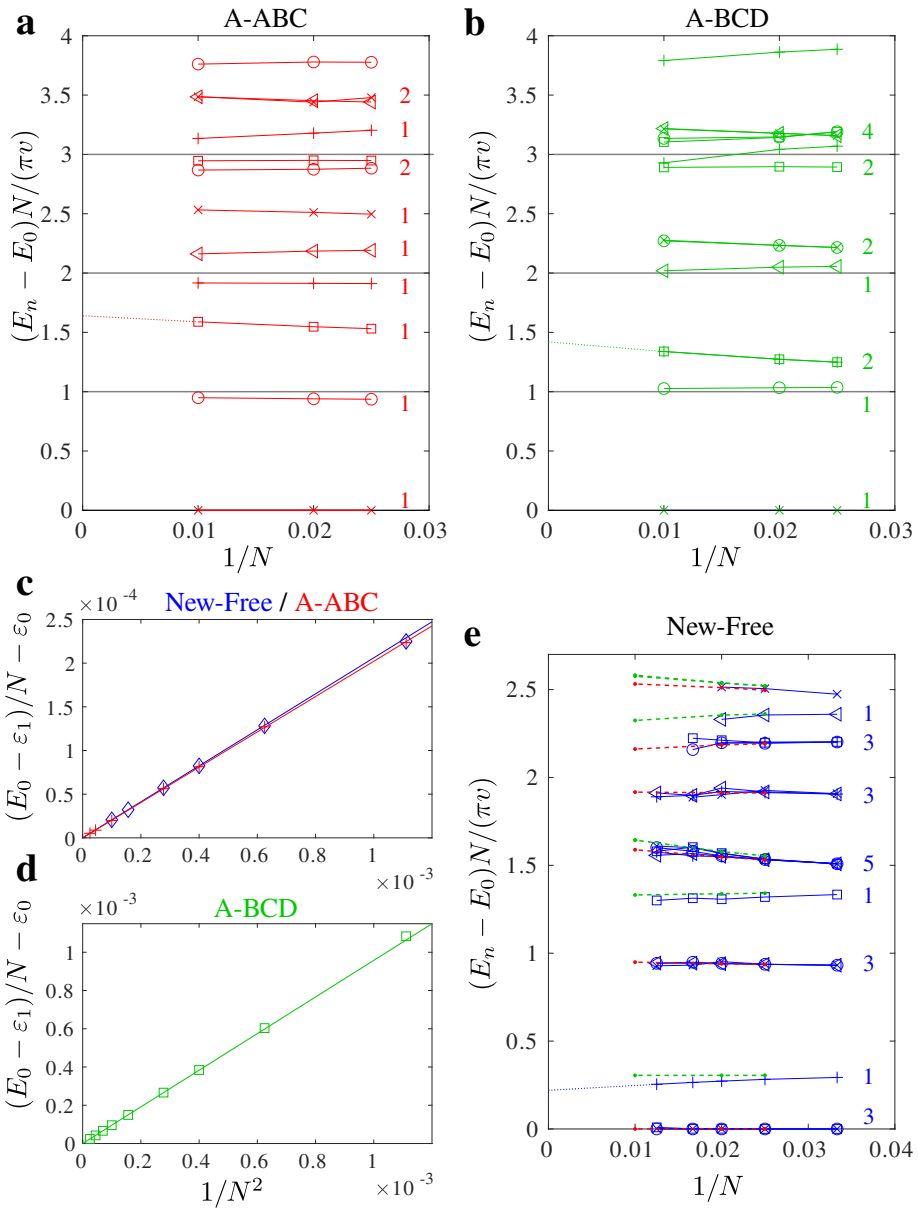

Figure 6: Conformal towers of states of the four-state Potts model with mixed **a** A-ABC and **b** A-BCD boundary conditions, and **e** with boundaries polarized in the direction of the transverse field (following Ref. [21] we use the term "new" boundary conditions). Symbols are DMRG data points extracted from the low-lying energy excitation spectra with velocity $v \approx 0.785$. Gray lines are the expected levels of the conformal towers with the smallest scaling dimension. In **e** the results from **a** (dashed red) and **b** (dashed green) are shown as a reference, the latter is shifted by $x = 1/24$. Dotted lines are finite-size extrapolations with a quadratic polynomial in $1/N$. **e** The numbers on the right side of the towers indicate the multiplicity of each energy level. **c-d** Finite-size scaling of the universal part of the ground-state energy fitted with Eq.14. **c** For ABC-ABC and New-New boundary conditions the extracted scaling dimension agrees within 4×10^{-3} with the expected value $x = 0$. **d** For the fixed ABC-ABD boundary conditions the scaling dimension of the primary field is close to $x = 1/24$ resulting in the data points of the order of 10^{-7}.

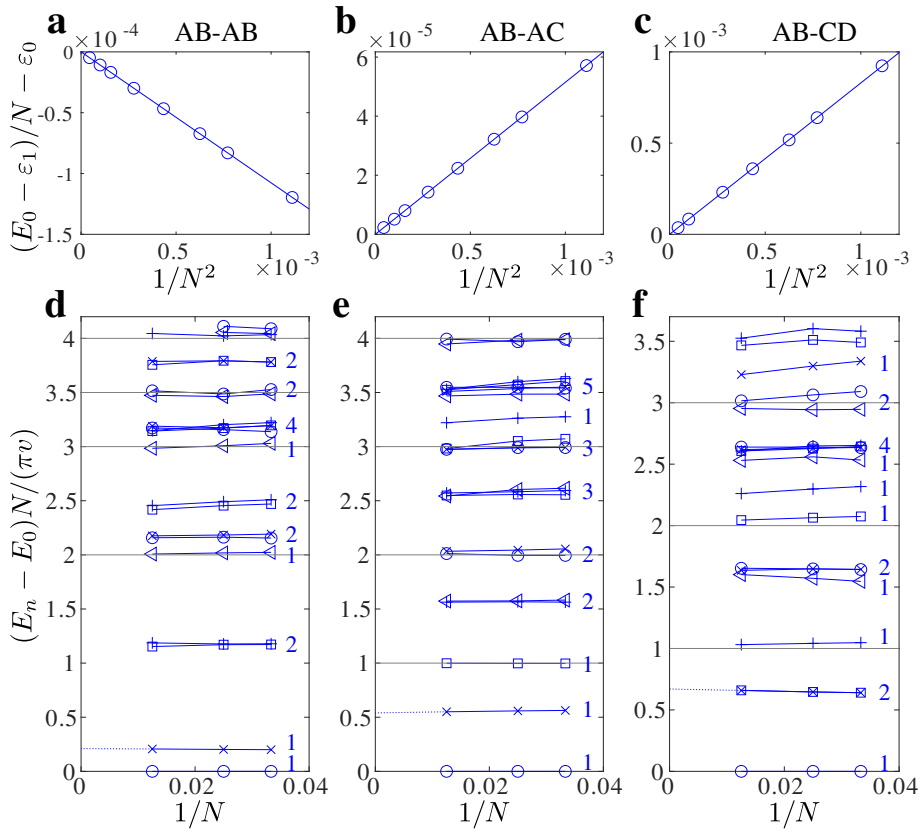

Figure 7: Finite-size scaling of the universal term in the ground-state energy (upper panels) and conformal tower of states (lower panels) of the four-state Potts model with two-state-mixed boundary conditions: **a, d** AB-AB; **b, e** AB-AC; and **c, f** AB-CD. Symbols are DMRG data points extracted from the low-lying energy excitation spectra with the velocity $v \approx 0.785$. The scaling dimension extracted from the ground-state in **a** agree with the identity tower $x = 0$ within 2×10^{-3}. **b** The lowest scaling dimension extracted numerically for AB-AC tower, $x \approx 0.0625$, is in excellent agreement with $x = 1/16$. **c** The scaling dimension of the AB-CD tower $x \approx 0.378$ points to $x = 3/8$ as a possible candidate. Gray lines are the expected levels of conformal towers with the smallest scaling dimensions (in **a** we also includes the double-degenerate primary with $x \approx 3.5$ as a part of the identity tower). Dotted lines in **d-f** are finite-size extrapolation (linear in $1/N$) of the lowest non-trivial energy levels.

conformal towers of states in the quantum three-state Potts model with fixed, mixed and free boundary conditions [15] and completes the numerical realization of all possible conformally-invariant boundary conditions for this model [21, 22].

The main message of the paper relies on the empirical observation that conformal towers of states of the quantum critical four-state Potts model with edges polarized in the direction of the transverse field can be expressed as a superposition of conformal towers of states with all possible combination of three-state-mixed boundary conditions. This establishes the duality between the transverse-polarized and the $(d-1)$-state-mixed boundary conditions, with one single-particle state suppressed at the edges. This generalizes previous predictions of the duality between the new and the two-state mixed boundary conditions [21] made for the three-state Potts critical theory. Furthermore, we also establish the duality between the fixed (A, B, C or D) and the free boundary conditions for the four-state Potts model. This suggests that the duality between these two sets of boundary

conditions is rather a generic feature. For Ising model the duality also holds, although the two pairs of boundary conditions are identical: an edge polarized in the direction of the transverse field is identical to free edge, while the $d-1$-state for $d=2$ naturally corresponds to the fixed (A or B) boundary conditions. This implies that the established duality holds at least at the two points on the Ashkin-Teller critical line: at the four-state Potts with $\lambda=1$; and at $\lambda=0$ that corresponds to the two decoupled Ising chains. It would thus be extremely interesting to see whether one can establish the duality for a generic Ashkin-Teller model with $0<\lambda<1$.

In addition, our results provide a phenomenological starting point for the boundary conformal field theory of the four-state Potts model. We empirically established the content of various conformal towers, in particular, the identity tower which on top of the zero-dimensional primary contains a double degenerate one of dimension $x\approx 3.5$. We detect the σ tower with conformal dimension $x=1/16$ which is known to be one of the "stable" conformal dimensions of the Ashkin-Teller theory and thus will remain the same for all values of λ. It would be very interesting to see whether the less obvious scaling dimensions obtained in the context of this work can be explained by means of boundary confornmal field theory. We hope that our numerical results will stimulate further analytical and numerical investigation of the boundary critical phenomena in the Ashkin-Teller model.

Acknowledgments

I would like to thank Frédéric Mila for stimulating questions that lead to investigation reported in this paper. I would also like to thank Frank Verstraete for pointing out that the "new" boundary conditions have been overlooked in our previous numerical study of the three-state Potts model. I am indebted to Ian Affleck for teaching me the basics of boundary conformal field theory in the context of other projects. Numerical simulations have been performed on the Dutch national e-infrastructure with the support of the SURF Cooperative and the facilities of the Scientific IT and Application Support Center of EPFL.

A Characters of the three-state Potts model

Six out of ten primary fields appear in the description of the operators identity I of zero dimension, magnetization σ of dimension $1/15$, energy ϵ of dimension $2/5$, and ψ of dimension $2/3$. The corresponding characters are:

$$\chi_I=\chi_{1,1}+\chi_{4,1} \qquad \chi_\epsilon=\chi_{2,1}+\chi_{3,1} \qquad \chi_\sigma=\chi_{\sigma^\dagger}=\chi_{2,3} \qquad \chi_\psi=\chi_{\psi^\dagger}=\chi_{1,3} \quad (30)$$

The small-q expansions of the characters for the ten primary fields of the three-state Potts minimal model are given by:

$$\chi_{(1,1)}(q) = q^{-1/30}\left(1+q^2+q^3+2q^4+2q^5+4q^6+...\right) \quad (31)$$
$$\chi_{(2,1)}(q) = q^{-1/30+2/5}\left(1+q+q^2+2q^3+3q^4+4q^5+6q^6+...\right) \quad (32)$$
$$\chi_{(3,1)}(q) = q^{-1/30+7/5}\left(1+q+2q^2+2q^3+4q^4+5q^5+8q^6+...\right) \quad (33)$$
$$\chi_{(4,1)}(q) = q^{-1/30+3}\left(1+q+2q^2+3q^3+4q^4+5q^5+8q^6+...\right) \quad (34)$$
$$\chi_{(1,2)}(q) = q^{-1/30+1/8}\left(1+q+q^2+2q^3+3q^4+4q^5+6q^6+...\right) \quad (35)$$
$$\chi_{(2,2)}(q) = q^{-1/30+1/40}\left(1+q+2q^2+3q^3+4q^4+6q^5+9q^6+...\right) \quad (36)$$
$$\chi_{(3,2)}(q) = q^{-1/30+21/40}\left(1+q+2q^2+3q^3+5q^4+7q^5+10q^6+...\right) \quad (37)$$
$$\chi_{(4,2)}(q) = q^{-1/30+13/8}\left(1+q+2q^2+3q^3+4q^4+6q^5+9q^6+...\right) \quad (38)$$
$$\chi_{(1,3)}(q) = q^{-1/30+2/3}\left(1+q+2q^2+2q^3+4q^4+5q^5+8q^6+...\right) \quad (39)$$
$$\chi_{(2,3)}(q) = q^{-1/30+1/15}\left(1+q+2q^2+3q^3+5q^4+7q^5+10q^6+...\right) \quad (40)$$

References

[1] J. L. Cardy, *Conformal invariance and surface critical behavior*, Nuclear Physics B **240**(4), 514 (1984), doi:https://doi.org/10.1016/0550-3213(84)90241-4.

[2] J. L. Cardy, *Boundary conditions, fusion rules and the verlinde formula*, Nuclear Physics B **324**(3), 581 (1989), doi:http://dx.doi.org/10.1016/0550-3213(89)90521-X.

[3] H. Saleur and M. Bauer, *On some relations between local height probabilities and conformal invariance*, Nuclear Physics B **320**(3), 591 (1989), doi:https://doi.org/10.1016/0550-3213(89)90014-X.

[4] I. Affleck and A. W. W. Ludwig, *Universal noninteger "ground-state degeneracy" in critical quantum systems*, Phys. Rev. Lett. **67**, 161 (1991), doi:10.1103/PhysRevLett.67.161.

[5] I. Affleck, *Conformal field theory approach to the kondo effect*, Acta Physica Polonica B (26), 1869 (1995), Cond-mat/9512099.

[6] E. Wong and I. Affleck, *Tunneling in quantum wires: A boundary conformal field theory approach*, Nuclear Physics B **417**(3), 403 (1994), doi:https://doi.org/10.1016/0550-3213(94)90479-0.

[7] J. L. Cardy, *Effect of boundary conditions on the operator content of two-dimensional conformally invariant theories*, Nuclear Physics B **275**(2), 200 (1986), doi:https://doi.org/10.1016/0550-3213(86)90596-1.

[8] I. Affleck, *Boundary condition changing operations in conformal field theory and condensed matter physics*, Nuclear Physics B - Proceedings Supplements **58**, 35–41 (1997), doi:10.1016/s0920-5632(97)00411-8.

[9] J. Cardy, *Boundary Conformal Field Theory*, arXiv e-prints hep-th/0411189 (2004), `hep-th/0411189`.

[10] I. Affleck, *Edge critical behaviour of the two-dimensional tri-critical ising model*, Journal of Physics A: Mathematical and General **33**(37), 6473 (2000), doi:10.1088/0305-4470/33/37/301.

[11] S. R. White, *Density matrix formulation for quantum renormalization groups*, Phys. Rev. Lett. **69**, 2863 (1992), doi:10.1103/PhysRevLett.69.2863.

[12] U. Schollwöck, *The density-matrix renormalization group*, Rev. Mod. Phys. **77**, 259 (2005), doi:10.1103/RevModPhys.77.259.

[13] S. Östlund and S. Rommer, *Thermodynamic limit of density matrix renormalization*, Phys. Rev. Lett. **75**, 3537 (1995), doi:10.1103/PhysRevLett.75.3537.

[14] U. Schollwöck, *The density-matrix renormalization group in the age of matrix product states*, Annals of Physics **326**(1), 96 (2011), doi:http://dx.doi.org/10.1016/j.aop.2010.09.012, January 2011 Special Issue.

[15] N. Chepiga and F. Mila, *Excitation spectrum and density matrix renormalization group iterations*, Phys. Rev. B **96**, 054425 (2017), doi:10.1103/PhysRevB.96.054425.

[16] G. Evenbly and G. Vidal, *Quantum Criticality with the Multi-scale Entanglement Renormalization Ansatz*, pp. 99–130, Springer Berlin Heidelberg, Berlin, Heidelberg, ISBN 978-3-642-35106-8, doi:10.1007/978-3-642-35106-8_4 (2013).

[17] A. M. Läuchli, *Operator content of real-space entanglement spectra at conformal critical points*, ArXiv e-prints (2013), 1303.0741.

[18] S. Iino, S. Morita and N. Kawashima, *Boundary conformal spectrum and surface critical behavior of classical spin systems: A tensor network renormalization study*, Phys. Rev. B **101**, 155418 (2020), doi:10.1103/PhysRevB.101.155418.

[19] N. Chepiga and F. Mila, *Dmrg investigation of constrained models: from quantum dimer and quantum loop ladders to hard-boson and fibonacci anyon chains*, SciPost Physics **6**(3) (2019), doi:10.21468/scipostphys.6.3.033.

[20] A. Rapp, P. Schmitteckert, G. Takács and G. Zaránd, *Asymptotic scattering and duality in the one-dimensional three-state quantum potts model on a lattice*, New Journal of Physics **15**(1), 013058 (2013).

[21] I. Affleck, M. Oshikawa and H. Saleur, *Boundary critical phenomena in the three-state potts model*, Journal of Physics A: Mathematical and General **31**(28), 5827–5842 (1998), doi:10.1088/0305-4470/31/28/003.

[22] J. Fuchs and C. Schweigert, *Completeness of boundary conditions for the critical three-state potts model*, Physics Letters B **441**(1), 141 (1998), doi:https://doi.org/10.1016/S0370-2693(98)01185-X.

[23] A. Kolezhuk, R. Roth and U. Schollwöck, *First order transition in the frustrated antiferromagnetic heisenberg $S = 1$ quantum spin chain*, Phys. Rev. Lett. **77**, 5142 (1996), doi:10.1103/PhysRevLett.77.5142.

[24] N. Chepiga, I. Affleck and F. Mila, *Dimerization transitions in spin-1 chains*, Phys. Rev. B **93**, 241108 (2016), doi:10.1103/PhysRevB.93.241108.

[25] N. Chepiga, I. Affleck and F. Mila, *Comment on "frustration and multicriticality in the antiferromagnetic spin-1 chain"*, Phys. Rev. B **94**, 136401 (2016), doi:10.1103/PhysRevB.94.136401.

[26] S. R. White, *Density-matrix algorithms for quantum renormalization groups*, Phys. Rev. B **48**, 10345 (1993), doi:10.1103/PhysRevB.48.10345.

[27] M. Chandross and J. C. Hicks, *Density-matrix renormalization-group method for excited states*, Phys. Rev. B **59**, 9699 (1999), doi:10.1103/PhysRevB.59.9699.

[28] R. J. Bursill, *Comment on "density-matrix renormalization-group method for excited states"*, Phys. Rev. B **63**, 157101 (2001), doi:10.1103/PhysRevB.63.157101.

[29] C. Degli Esposti Boschi and F. Ortolani, *Investigation of quantum phase transitions using multi-target dmrg methods*, The European Physical Journal B - Condensed Matter and Complex Systems **41**(4), 503 (2004), doi:10.1140/epjb/e2004-00344-1.

[30] I. P. McCulloch, *From density-matrix renormalization group to matrix product states*, Journal of Statistical Mechanics: Theory and Experiment **2007**(10), P10014 (2007).

[31] D. Porras, F. Verstraete and J. I. Cirac, *Renormalization algorithm for the calculation of spectra of interacting quantum systems*, Phys. Rev. B **73**, 014410 (2006), doi:10.1103/PhysRevB.73.014410.

[32] V. S. Dotsenko, *Critical Behavior and Associated Conformal Algebra of the Z(3) Potts Model*, Nucl. Phys. **B235**, 54 (1984), doi:10.1016/0550-3213(84)90148-2.

[33] H. N. V. Temperley and E. H. Lieb, *Relations between the 'percolation' and 'colouring' problem and other graph-theoretical problems associated with regular planar lattices: some exact results for the 'percolation' problem*, Proc. Roy. Soc. Lond. **A322**, 251 (1971), doi:10.1098/rspa.1971.0067.

[34] P. Francesco P., Mathieu and Sénéchal, *Conformal field theory* (1997).

[35] J. Ashkin and E. Teller, *Statistics of two-dimensional lattices with four components*, Phys. Rev. **64**, 178 (1943), doi:10.1103/PhysRev.64.178.

[36] S.-K. Yang, *Modular invariant partition function of the ashkin-teller model on the critical line and n = 2 superconformal invariance*, Nuclear Physics B **285**, 183 (1987), doi:https://doi.org/10.1016/0550-3213(87)90334-8.

[37] M. Oshikawa and I. Affleck, *Boundary conformal field theory approach to the critical two-dimensional ising model with a defect line*, Nuclear Physics B **495**(3), 533–582 (1997), doi:10.1016/s0550-3213(97)00219-8.

[38] N. Chepiga and F. Mila, *Kibble-zurek exponent and chiral transition of the period-4 phase of rydberg chains*, Nature Communications **12**(1) (2021), doi:10.1038/s41467-020-20641-y.

[39] N. Chepiga, *Dimerization and exotic criticality in spin-s chains*, EPFL thesis **7621**, 184 (2017), doi:10.5075/epfl-thesis-7621.